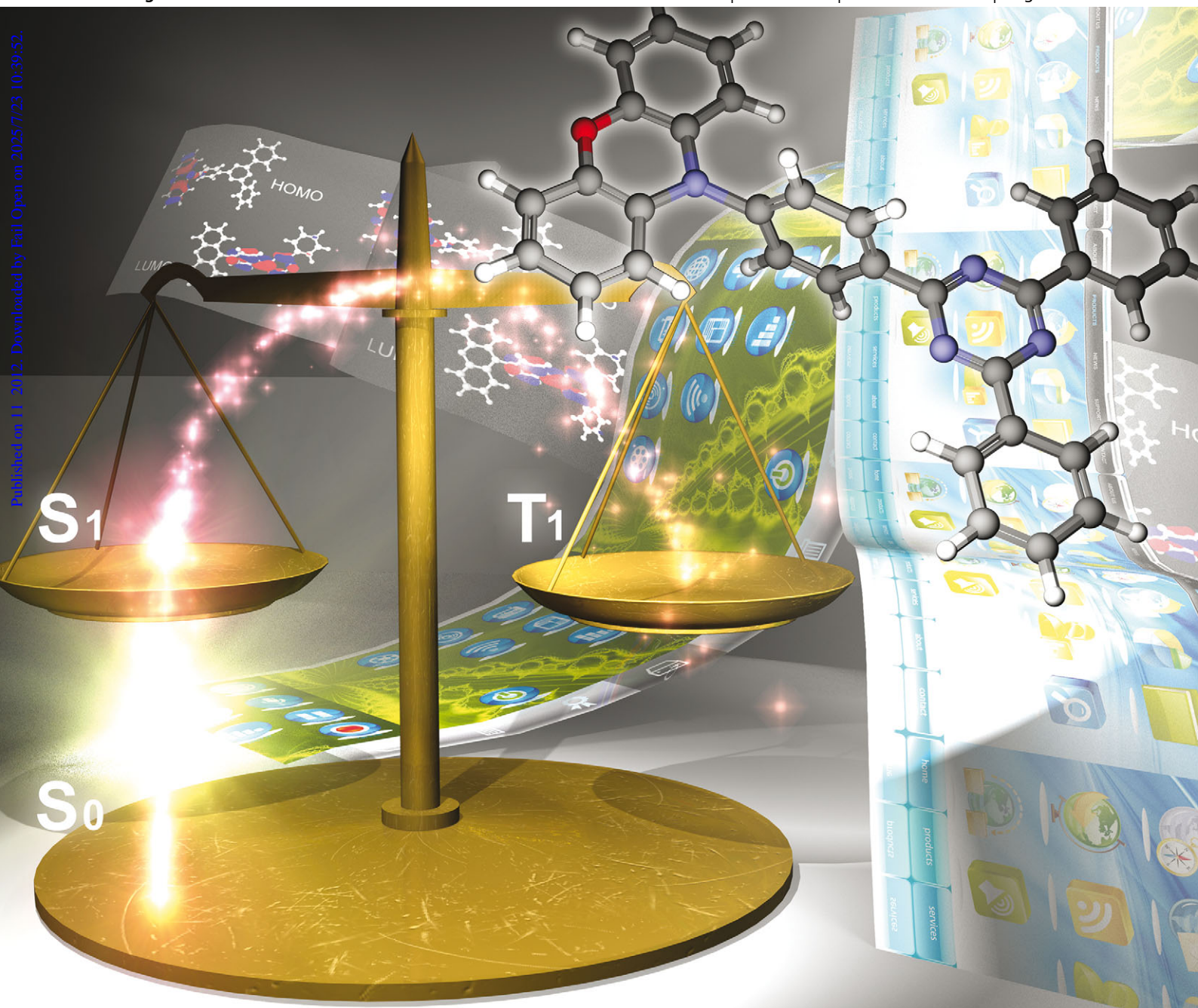


ChemComm

Chemical Communications

www.rsc.org/chemcomm

Volume 48 | Number 93 | 4 December 2012 | Pages 11369–11468



ISSN 1359-7345

RSC Publishing

COMMUNICATION

Chihaya Adachi *et al.*,
Efficient green thermally activated delayed fluorescence (TADF) from a
phenoxazine-triphenyltriazine (PXZ-TRZ) derivative



1359-7345(2012)48:93;1-R

Cite this: *Chem. Commun.*, 2012, **48**, 11392–11394

www.rsc.org/chemcomm

COMMUNICATION

Efficient green thermally activated delayed fluorescence (TADF) from a phenoxazine–triphenyltriazine (PXZ–TRZ) derivative†Hiroyuki Tanaka,^a Katsuyuki Shizu,^a Hiroshi Miyazaki^{ab} and Chihaya Adachi^{*a}

Received 28th August 2012, Accepted 24th September 2012

DOI: 10.1039/c2cc36237f

Efficient thermally activated delayed fluorescence (TADF) was developed in a material based on a phenoxazine (PXZ) electron donor unit and a 2,4,6-triphenyl-1,3,5-triazine (TRZ) electron acceptor unit. An organic light-emitting diode containing this novel TADF emitter layer was fabricated and exhibited a maximum external quantum efficiency of 12.5% with green emission.

Since Tang and VanSlyke reported the first practical multi-layered organic electroluminescent (EL) device in 1987,¹ the research area of organic light-emitting diodes (OLEDs) has developed rapidly and OLEDs have been applied to advanced flat-panel displays. In particular, the development of OLED luminescent materials is an important issue and these materials have been classified into two major categories. The first is fluorescent materials, which can harvest only the singlet excitons (25%) that are generated by electrical excitation. The second is phosphorescent materials, which can harvest the triplet excitons generated (75%). The branching ratio of singlet and triplet excitons is 1 : 3, which is limited by a spin statistics rule.² Therefore, in recent devices, phosphorescent materials and their related technologies have been indispensable to obtain high EL efficiency. However, phosphorescent materials generally contain a rare metal element such as Ir or Pt. These metals are rather expensive and are dependent on limited global resources. Therefore, we recently proposed the alternative idea of TADF as a third generation-luminescent material, instead of the conventional fluorescent and phosphorescent materials, which can realize the ultimate EL efficiency by efficient up-conversion from the lowest triplet excited state (T_1) to the lowest singlet excited state (S_1) through reverse intersystem crossing (RISC).³ The up-conversion from T_1 to S_1 can be classified into two types of possible mechanisms. One possible mechanism is triplet–triplet annihilation (TTA)⁴ and the other is TADF.⁵ In the TTA mechanism, S_1 or T_1 results from fusion between two triplet excitons, and depends on the molecular packing

style in the emission layers.⁶ The additional singlet exciton production can increase the internal quantum efficiency (η_{int}) up to 15% or 37.5% depending on the up-conversion mechanism.^{7–10} Therefore, η_{int} can be increased up to 40% or 62.5%. In contrast to the TTA mechanism, the TADF strongly depends on HOMO–LUMO separation in a single molecule. TADF materials have a sufficiently small energy gap between S_1 and T_1 (ΔE_{ST}) to enable up-conversion of the triplet exciton from T_1 to S_1 . This small ΔE_{ST} enables TADF materials to realize 100% of the exciton formation generated by electrical excitation at S_1 .

In this communication, we propose a novel TADF emitter PXZ–TRZ. Details of the synthesis scheme are given in ESI.† TADF materials must have an effective separation of HOMO and LUMO in a single molecule to obtain a near-zero-energy gap between S_1 and T_1 and the effective separation induces charge transfer (CT) transition from HOMO to LUMO. To realize the effective separation, we introduced a twisted structure into the molecule by selecting PXZ instead of carbazole, as the donor unit. While carbazole units have been widely used as donor units in OLEDs, we found that the PXZ unit provides a unique molecular geometry in the PXZ–TRZ structure that matches our TADF molecular design. Compared with carbazole, which has a five-membered ring in the fused ring, PXZ has a morpholine-like six-membered ring, which causes steric repulsion toward any neighbor substituents. Therefore, PXZ can easily achieve an effective separation of HOMO and LUMO to induce the CT transition.¹¹ The oxygen atom of PXZ also works to localize the electron density-distribution of HOMO on the PXZ donor unit. On the basis of density functional theory (DFT) calculation, X-ray structural analysis, photophysical properties and OLED characteristics, we discuss the molecular design and TADF characteristics.

As mentioned above, an effective separation of the spatial distribution of the HOMO and LUMO is essential for realization of a small ΔE_{ST} and thus enhanced RISC.³ One possible way to achieve the effective HOMO–LUMO separation is to twist a donor–acceptor system and interfere with the π -conjugation. The molecular design of PXZ–TRZ is based on this concept. PXZ acts as a donor, while TRZ acts as an acceptor. For PXZ–TRZ, steric repulsion between the hydrogen atoms at the donor–acceptor linkage leads to a large dihedral angle between the donor and acceptor planes (estimated to be 74.9° from the X-ray structure). To investigate the properties of the excited states of PXZ–TRZ, we performed quantum chemical calculation of

^a Center for Organic Photonics and Electronics Research (OPERA), Kyushu University, 744 Motoooka, Nishi, Fukuoka 819-0395, Japan. E-mail: adachi@cstf.kyushu-u.ac.jp; Fax: +81-92-802-6921; Tel: +81-92-802-6920

^b Functional Materials Laboratories, Nippon Steel Chemical Co., Ltd., 46-80 Nakabaru, Sakinohama, Tobata, Kitakyushu, Fukuoka 804-8503, Japan

† Electronic supplementary information (ESI) available: Synthesis scheme, experimental details, crystallographic data and additional photophysical data. CCDC 893246. For ESI and crystallographic data in CIF or other electronic format see DOI: 10.1039/c2cc36237f

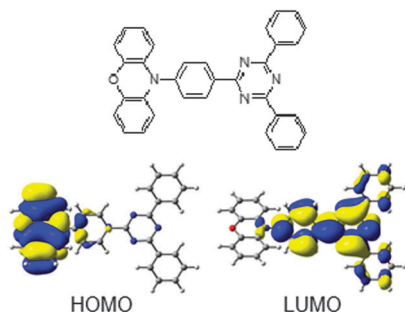


Fig. 1 Molecular structures and HOMO and LUMO of PXZ-TRZ calculated at the PBE0/6-31G level.

the low-lying excited states of this compound using time-dependent density functional theory (TD-DFT). First, the ground-state geometry was optimized with Gaussian 09 software¹² using the PBE0 hybrid functional¹³ and the 6-31G(d) basis set.¹⁴ Then, the ten lowest singlet and triplet excited states were calculated by the TD-DFT method at their optimized ground-state geometries using the same functional and basis set. The geometrical parameters of the optimized ground state agree well with those derived from the X-ray structure: the dihedral angle between the donor and acceptor planes is calculated to be 74.8°, which is in good agreement with the measured value of 74.9°. Fig. 1 shows the HOMO and LUMO of PXZ-TRZ. The HOMO is mainly distributed on the PXZ moiety, while the LUMO is localized on the TRZ moiety. There is a small overlap in the phenyl ring connecting PXZ and TRZ. The calculated S_1 and T_1 correspond to CT states: an electron moves from PXZ to TRZ. Because the overlap between the HOMO and the LUMO is small, an exchange interaction between two electrons in the HOMO and the LUMO is effectively suppressed, and consequently ΔE_{ST} is quite small. The ΔE_{ST} value for PXZ-TRZ was calculated to be 0.070 eV, which is smaller than that calculated for PIC-TRZ (0.252 eV) with the same method. The small ΔE_{ST} value of PXZ-TRZ induces efficient up-conversion from the T_1 state to the S_1 state through the RISC, and increases the emission quantum yield.

To verify the optimized structure estimated by the DFT calculation, we conducted single-crystal X-ray structural analysis of PXZ-TRZ. Fig. 2 shows the asymmetric unit of PXZ-TRZ (details of the crystal structure analysis are shown in Fig. S1 in the ESI†). The TRZ moiety was almost co-planar. The dihedral angle between the PXZ moiety and the phenyl ring connecting the donor and acceptor units was 74.9°, which was caused by steric repulsion between the hydrogen atoms. The molecular structure determined almost corresponded to the optimized structure estimated from the DFT calculation. This twisted structure suppresses the spread of electron density distribution from the PXZ

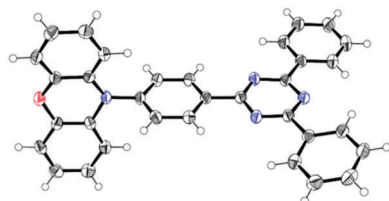


Fig. 2 ORTEP drawing of PXZ-TRZ. Thermal ellipsoids are drawn at the 50% probability level.

moiety to the triazine moiety and induces efficient separation of the HOMO and the LUMO.

Electron transfer derived from the donor-acceptor separation of TADF materials can be confirmed by the CT transition on the UV-vis absorption spectrum. The UV-vis absorption and photoluminescence (PL) spectra of PXZ-TRZ in a toluene solution are shown in Fig. S2 (ESI†). A broad absorption peak at around 420 nm was observed. This peak can be assigned to the CT transition from the PXZ moiety to the TRZ moiety. The PL spectrum of PXZ-TRZ was observed by excitation at the absorption peak of 420 nm derived from the CT transition. The peak wavelength was 545 nm and the fluorescence was pure green. The CIE color coordinate was $x = 0.34$ and $y = 0.57$. To experimentally confirm the small ΔE_{ST} estimated by the TD-DFT calculation, we performed low temperature PL measurements (Fig. S3, ESI†). A significant overlap was observed between the prompt and delayed spectra (at 77 K). This result clearly indicates that the ΔE_{ST} of PXZ-TRZ is very small. To verify the up-conversion from T_1 to S_1 , we conducted PL lifetime measurements in the toluene solution. To prevent inactivation from T_1 to the triplet ground state of oxygen molecules, deoxygenation by nitrogen bubbling was carried out. The PL quantum yield (Φ_{PL}) was increased from 14.5% to 29.5% by the deoxygenation. Fig. 3 shows the transient PL decay profile of PXZ-TRZ. The transient decay can be classified into two components. The first is a prompt component from S_1 to the singlet ground state (S_0), which is a nanosecond-order decay. The second is a delayed component from T_1 to S_0 through S_1 , which is caused by successive RISC and up-conversion. The decay shows as 19 ns for the prompt component and 0.676 μ s for the delayed component. To confirm that the observed delayed component is TADF and not a delayed fluorescence derived from TTA, we investigated the temperature dependence of the PL spectrum of a 6 wt% doped film of PXZ-TRZ in 4,4'-bis(*N*-carbazolyl)-1,1'-biphenyl (CBP) using a streak camera (Fig. S4 and S5, ESI†). With a rise in temperature from 50 K, the PL quantum efficiency of the delayed component gradually increased and reached 17% at 300 K. On the other hand, that of the prompt component was almost constant at around 50%. From these results, we confirmed that PXZ-TRZ is a TADF material.

We fabricated an OLED containing PXZ-TRZ as a TADF emitter. The device structures are ITO/*N,N'*-diphenyl-*N,N'*-bis(1-naphthyl)-1,10-biphenyl-4,4'-diamine (α -NPD) (35 nm)/6 wt%-PXZ-TRZ:CBP (15 nm)/TPBI (65 nm)/LiF (0.8 nm)/Al (80 nm).

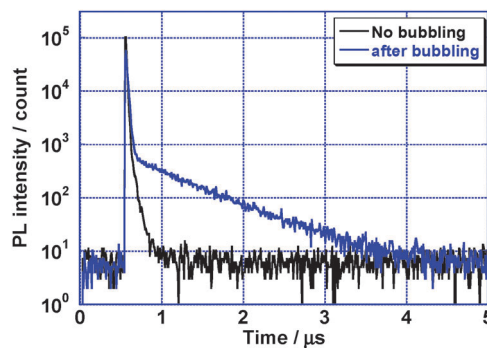


Fig. 3 Transient PL decay profile of PXZ-TRZ in 10^{-5} M toluene solution. Black and blue lines show the profiles before and after the deoxygenation, respectively.

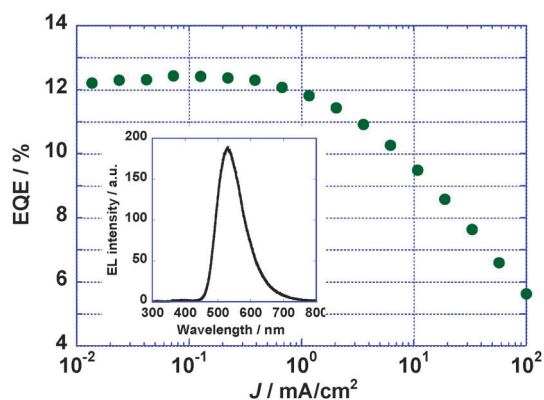


Fig. 4 (a) Dependence of EQE on current density for the OLED with the structure ITO/a-NPD (35 nm)/6 wt% PXZ–TRZ:CBP (15 nm)/TPBi (65 nm)/LiF (0.8 nm)/Al (80 nm). Inset: EL spectrum of the OLED containing PXZ–TRZ.

The HOMO and LUMO levels were determined to be 5.5 eV and 3.1 eV from the results of the UV-vis absorption spectrum of the neat films and the work function measurement,¹⁵ respectively. Because the HOMO and LUMO levels of PXZ–TRZ are located inside those levels of a CBP layer, it would be reasonable to assume that direct carrier injection (both electron and hole) occurs from the adjacent carrier transport layers (Fig. S6, ESI†). The Φ_{PL} of a 6 wt% doped film of PXZ–TRZ in a CBP layer was 65.7%, which was increased to approximately double that value obtained in the toluene solution, indicating that the concentration quenching process with non-radiative decay was well suppressed in the doped film. The OLED characteristics of PXZ–TRZ are shown in Fig. 4. The green EL spectrum was observed at around 529 nm, as shown in the inset of Fig. 4. The external quantum efficiency (EQE) vs. current density plot demonstrated a maximum EQE (EQE_{max}) of 12.5%. This result is beyond the theoretical limit if we assume that PXZ–TRZ is a normal fluorescent emitter. EQE_{max} should be 5–7% with the assumption of an out-coupling efficiency of 0.2–0.3. This phenomenon indicates the amplification of the singlet excitons derived from the up-conversion from T_1 to S_1 by realization of the small ΔE_{ST} . From the results of the temperature dependence of the PL spectrum, we estimated the theoretical value of EQE_{max} using the equation shown below:^{3b} where η_{int} is the internal quantum efficiency, η_{out} is the out-coupling constant, γ is the ratio of the charge injection to the electron and hole transportation, η_r is the excitation–production ratio, ϕ_p is the photoluminescent quantum yield of the prompt component, and ϕ_d is the photoluminescent quantum yield of the delayed component. At 300 K, η_{ext} was

$$\begin{aligned} \eta_{\text{ext}} &= \eta_{\text{int}}\eta_{\text{out}} = \gamma\eta_r\eta_{\text{PL}}\eta_{\text{out}} \\ &= \gamma \times \left[0.25 \times \phi_{\text{prompt}} + \{0.75 + 0.25(1 - \phi_p)\} \frac{\phi_d}{1 - \phi_p} \right] \\ &\quad \times \eta_{\text{out}} \end{aligned} \quad (1)$$

estimated to be 12%, where γ , η_{out} , ϕ_p , and ϕ_d are 1.0, 0.3, 0.49 and 0.17, respectively. The estimated value corresponded well with the observed EQE_{max} . Although a roll-off of the EQE was

observed at higher current densities, the maximum luminance reached nearly 10000 cd m^{-2} (Fig. S7, ESI†).

In summary, we designed and synthesized a novel TADF emitter, PXZ–TRZ, which has a very small ΔE_{ST} , inducing both efficient up-conversion from T_1 to S_1 and an intense fluorescence that leads to high EL efficiency. PXZ is a useful and typical electron-donor unit, which can rationally create an efficient TADF emitter. The prediction of the frontier orbital by quantum chemical calculation is a powerful method to create an efficient TADF emitter and our calculations are consistent with the experimental results of the X-ray structural analysis and with the photophysical properties. PXZ–TRZ is the first green fluorescence emitter with a high EQE_{max} of over 12%. By selecting a better donor–acceptor pair to improve the PL quantum efficiency, we believe that TADF materials will show the potential to surpass the performance of phosphorescent materials.

This research is funded by a grant from the Japan Society for the Promotion of Science (JSPS) through the ‘‘Funding Program for World-Leading Innovative R&D on Science and Technology (FIRST Program)’’. The authors acknowledge Ms H. Nomura and Ms N. Nakamura for performing the measurements of the thermal analysis (TG-GTA and DSC) and sublimation, and Mr T. Matsumoto for the single-crystal X-ray crystal structural analysis.

Notes and references

- 1 C. W. Tang and S. A. VanSlyke, *Appl. Phys. Chem.*, 1987, **51**, 913.
- 2 (a) M. A. Baldo, D. F. O’Brien, M. E. Thompson and S. R. Forrest, *Phys. Rev. B: Condens. Matter Mater. Phys.*, 1999, **60**, 14422; (b) M. Segal, M. A. Baldo, R. J. Holmes, S. R. Forrest and Z. G. Soos, *Phys. Rev. B: Condens. Matter Mater. Phys.*, 2003, **68**, 075211; (c) B. H. Wallikewitz, D. Kabra, S. Gelinas and R. H. Friend, *Phys. Rev. B: Condens. Matter Mater. Phys.*, 2012, **85**, 045209; (d) T. Tsutsui, *MRS Bull.*, 1997, **22**, 39.
- 3 (a) A. Endo, M. Ogasawara, A. Takahashi, D. Yokoyama, Y. Kato and C. Adachi, *Adv. Mater.*, 2009, **21**, 4802; (b) A. Endo, K. Sato, K. Yoshimura, T. Kai, A. Kawada, H. Miyazaki and C. Adachi, *Appl. Phys. Lett.*, 2011, **98**, 083302; (c) T. Nakagawa, S.-Y. Ku, K.-T. Wong and C. Adachi, *Chem. Commun.*, 2012, **48**, 9580.
- 4 J. B. Birks, *Photophysics of Organic Molecules*, Wiley, New York, 1970, p. 372.
- 5 B. Valeur, *Molecular Fluorescence*, Wiley-VCH, Weinheim, 2002, p. 41.
- 6 H. Fukagawa, T. Shimizu, N. Ohbe, S. Tokito, K. Tokumaru and H. Fujikake, *Org. Electron.*, 2012, **13**, 1197.
- 7 D. Y. Kondakov, T. D. Pawlik, T. K. Hatwar and J. P. Spindler, *J. Appl. Phys.*, 2009, **106**, 124510.
- 8 C. T. Brown and D. Y. Kondakov, *J. Soc. Inf. Disp.*, 2004, **12**, 323.
- 9 D. Y. Kondakov, *J. Soc. Inf. Disp.*, 2009, **17**, 137.
- 10 D. Y. Kondakov, *J. Appl. Phys.*, 2007, **102**, 114504.
- 11 P. Borowicz, J. Herbich, A. Kapturkiewicz, M. Opallo and J. Nowacki, *Chem. Phys.*, 1999, **249**, 49.
- 12 M. J. Frisch *et al.*, *GAUSSIAN 09, Revision B.01*, Gaussian, Inc., Wallingford, CT, 2009.
- 13 C. Adamo and V. Barone, *J. Chem. Phys.*, 1999, **110**, 6158.
- 14 P. C. Hariharan and J. A. Pople, *Theor. Chim. Acta*, 1973, **28**, 213.
- 15 The experimental HOMO energy level of the neat film was determined to be 5.5 eV using a Riken-Keiki AC-2 photoelectron spectrometer; the LUMO energy level was estimated to be 3.1 eV by subtracting the optical energy gap (2.4 eV) estimated from the UV-vis absorption spectrum from the measured HOMO energy level.